The Proteome of Central and Peripheral Retina with Progression of Age-Related Macular Degeneration

Cheryl M. Ethen,[1] *Cavan Reilly,*[2] *Xiao Feng,*[3] *Timothy W. Olsen,*[3] *and Deborah A. Ferrington*[3]

Purpose. A growing understanding of the molecular events in age-related macular degeneration (AMD) has lead to targeted therapies for a select group of patients with advanced AMD. Development of therapies for the earlier stages requires further elucidation of disease mechanisms. In this study, a proteomics approach was used to identify proteins that had altered content in human donor eyes with progression of AMD.

Methods. The early molecular events associated with AMD were identified by comparing the proteome of the macular and peripheral neurosensory retina during four progressive stages of AMD. Proteins were resolved and quantified by two-dimensional gel electrophoresis. Twenty-six proteins exhibited changes in content and were identified by matrix-assisted laser desorption ionization—time of flight (MALDI-TOF) mass spectrometry. Two-dimensional (2-D) and semiquantitative one-dimensional (1-D) Western blot analyses were used to determine whether changes identified by proteomic analysis were specific for a protein subpopulation or representative of the entire protein population.

Results. Twenty-six proteins were identified that exhibited changes at disease onset or with progression (indicating potential causal mechanisms) and at end-stage disease (indicating potential secondary consequences). These proteins are involved in key functional pathways, such as microtubule regulation and protection from stress-induced protein unfolding. Approximately 60% of the proteins exhibited changes specific to either the macula or periphery, with the remaining 40% changing in both regions. These results imply that both the macula and periphery are affected by AMD.

Conclusions. This study provides the first direct evidence of AMD stage- and region-specific changes in retinal protein levels and highlights potential novel, disease-related proteins and biochemical pathways for future studies of AMD. (*Invest Ophthalmol Vis Sci.* 2006;47:2280–2290) DOI:10.1167/iovs.05-1395

Age-related macular degeneration (AMD) is the leading cause of vision loss and blindness in individuals over age 60 in the developed world.[1,2] This disorder is characterized by the loss of central vision caused by pathologic aging of the macula. Treatments for AMD are rapidly evolving and some newer therapies now target specific biochemical events. For end-stage neovascular AMD, the use of photodynamic therapy[3,4] and pharmacotherapy targeting the increased expression of vascular endothelial growth factor (VEGF)[5] have been shown to attenuate vision loss. Although progress is being made in the management of discrete subpopulations of patients with AMD, treatments for most individuals with AMD remain limited. The continued development of therapeutic strategies requires a greater understanding of the genetic and molecular events associated with AMD.

AMD is a complex disorder involving multiple anatomic layers including the neurosensory retina containing photoreceptors and six other cell layers, the retinal pigment epithelium (RPE), the underlying Bruch's membrane, and the highly vascular choroid. Although each of these tissues has been implicated in AMD pathogenesis,[6–10] this study focused on the neurosensory retina. Several lines of evidence provide the rationale for our focus. For example, the degeneration of rod photoreceptors precedes RPE atrophy and drusen formation.[11–14] Many clinical features presented in AMD are also seen in patients with a mutation in the peripherin/retinal degeneration slow (RDS) gene that encodes a photoreceptor-specific protein.[15] Furthermore, macular translocation causes recurring neovascularization or geographic atrophy in the RPE and choroid underlying the translocated macula,[16–18] suggesting that factors originating from the neurosensory retina potentially stimulate either apoptosis or angiogenesis.

Another clinical finding in AMD that warrants further investigation is the apparent greater susceptibility of the macula to degeneration when compared with the peripheral retina. This susceptibility can be partially explained by anatomic and physiological differences between the two regions. For example, the population of photoreceptors is clearly distinct in each region; the macula contains a proportionately higher density of cones than does the periphery.[9] The increased metabolic activity, elevated blood flow in the choroid, and exposure to focused light energy also distinguish the macula from the periphery.[19] Although these differences have been well described, further investigations to explain the molecular basis for the region-specific differences in susceptibility to degeneration are needed.

In the present study, we performed a detailed comparison of the neurosensory retina proteome from the macula and periphery during progression of AMD. Human donor eyes were categorized into four progressive stages of AMD using the Minnesota Grading System (MGS).[20] The MGS uses the criteria from the Age-Related Eye Disease Study (AREDS),[1,21] considered to be the standard in clinical studies of AMD, and is based on clinical definitions from large epidemiologic studies.[22] Our

From the Departments of [1]Biochemistry, Molecular Biology, and Biophysics and [3]Ophthalmology, and the [2]Division of Biostatistics, University of Minnesota, Minneapolis, Minnesota.

Supported in part by Grants EY014176 (DAF) and AG025392 (TWO) from the National Institutes of Health, a Career Development Award from the American Federation for Aging Research and Foundation Fighting Blindness (DAF), the American Health Assistance Foundation, Minnesota Medical Foundation, the University of Minnesota Academic Health Center and Graduate School, the Fesler-Lampert Foundation, and an unrestricted grant to the Department of Ophthalmology from the Research the Prevent Blindness Foundation. CME was supported by a Training Grant in Vision Science T32-EY07133 from the National Eye Institute.

Submitted for publication October 26, 2005; revised December 22, 2005, and February 13, 2006; accepted April 21, 2006.

Disclosure: **C.M. Ethen**, None; **C. Reilly**, None; **X. Feng**, None; **T.W. Olsen**, None; **D.A. Ferrington**, None

The publication costs of this article were defrayed in part by page charge payment. This article must therefore be marked "*advertisement*" in accordance with 18 U.S.C. §1734 solely to indicate this fact.

Corresponding author: Deborah A. Ferrington, 380 Lions Research Building, 2001 6th Street SE, Minneapolis, MN 55455; ferri013@umn.edu.

Copyright © Association for Research in Vision and Ophthalmology

Downloaded from iovs.arvojournals.org on 08/15/2022

grading system thus provides a unique opportunity for distinguishing protein changes occurring at early disease stages, potentially reflecting causal mechanisms, from changes that occur in end-stage disease, potentially reflecting secondary effects of AMD. By using comparative proteomic analysis, including high-resolution two-dimensional (2-D) protein electrophoresis, mass spectrometry (MS), and 2-D and one-dimensional (1-D) Western blot (WB), we performed a comprehensive investigation of protein-specific changes occurring at progressive stages of AMD. This information narrows the focus for future investigations to examine specific proteins and biochemical pathways that are relevant to AMD progression.

METHODS

Grading Donor Eyes

Eyes obtained from the Minnesota Lions Eye Bank were acquired with the consent of the donor or donor family to be used for medical research in accordance with the principals outlined in the Declaration of Helsinki. After enucleation, eyes were maintained at 4°C in a moist chamber until dissection and photographing were achieved. Dissection of the sensory retina was performed as reported previously.[23] Criteria established by the MGS were used to determine the stage of AMD.[20] The stages of AMD are referred to as MGS1 (minimal or no AMD) through MGS4 (severe AMD), corresponding directly with the AREDS classification system.[21] MGS1 represents our control group and includes individuals with either no or a few, small drusen. MGS2 is considered an early stage of AMD (i.e., having more numerous small drusen and possible pigmentary changes). The most clinically relevant change in prognosis for future vision loss occurs from AREDS categories 2 to 3. These categories correspond to the change from MGS2 to -3. MGS3 is defined primarily by numerous intermediate sized drusen or noncentrally located geographic atrophy. Advanced AMD (MGS4) corresponds to central macular damage from either geographic atrophy (atrophic AMD), or active choroidal neovascularization (exudative AMD). In the present study, all MGS4 samples were exudative AMD. Based on clinical examination of the neurosensory tissue, donor eyes were screened for and excluded if other ocular diseases were observed clinically, such as glaucoma or diabetic retinopathy.

Preparation of Retinal Homogenates

Retinal homogenates were prepared as described.[23] In brief, a trephine punch of 8-mm diameter was centered over the macular area to separate the macula from the periphery. The neurosensory retina was then carefully peeled away from the RPE layer and homogenized (~15 passes in a glass homogenizer with a Teflon pestle) in buffer containing 20% sucrose, 20 mM Tris-acetate (pH 7.2), 2 mM $MgCl_2$, 10 mM glucose, and 2% CHAPS (3-([3-cholamidopropyl]dimethylammonio-2-hydroxy-1-propanesulfonate). The retinal homogenates were then centrifuged at 100*g*, the supernantant retained, the pellet rehomogenized, and both supernatants combined before centrifugation at 600*g*. The supernatant from the final spin was stored at −80°C. Protein concentrations were determined using the bicinchoninic acid (BCA) protein assay reagents (Pierce Biotechnology, Rockford, IL). Bovine serum albumin was used as a standard.

Rat Retinal Protein Stability

Five-month-old Fischer 344 rats were purchased from the Veterinary Medical Unit at the Minneapolis Veterans Affairs Medical Center's aging rodent colony, which is maintained by the University of Minnesota. An animal protocol was approved by the Institutional Animal Care and Use Committee of the University of Minnesota and followed guidelines established by the Association for Research in Vision and Ophthalmology. In these experiments, the conditions of human donor eyes were replicated to mimic eye bank conditions. For example, bodies were maintained at room temperature for 2.5 hours then refrigerated until enucleation at 4.5 hours after death. After enucleation, eyes were stored in a moist chamber until retinal dissection was performed. Two rats were used for each time point. After rats were euthanized with carbon dioxide, one eye from each rat was immediately enucleated, and retinas were dissected and frozen at −80°C. Eyes processed immediately after death served as the control for the remaining eyes that were dissected at one of six time points ranging from 2 to 12 hours postmortem. Frozen retinas from two rat eyes were combined and processed as outlined for human retinas. Retinal proteins were resolved by 1-D SDS-PAGE. Protein profiles from each time point were aligned and quantitated used Quantity One software (Bio-Rad, Hercules, CA) comparing the control retinas with their companions harvested at a later time after death. Two separate experiments gave identical results.

TABLE 1. Antibody Information

Primary Antibody	Type*	Dilution	Company
HSP60	M	1:2500	BD Biosciences, San Jose, CA
α-tubulin	M	1:5000	Abcam, Cambridge, MA
HOP	M	1ug/ml	StressGen, Victoria, BC, Canada
VDAC	M	3ug/ml	Calbiochem, San Diego, CA
CRABP	M	1:1000	Sigma-Aldrich, St. Louis, MO
Prefoldin-1	P	1:500	Genway, San Diego, CA
Enolase	P	1:200	BioDesign, Saco, ME
GRP78/BiP	P	1:3000	Santa Cruz, Santa Cruz, CA
GUK1	P	1:3000	Abnova, Taipei City, Taiwan
Stathmin	P	1:1000	Cell Signaling, Beverly, MA
ERp29	P	1:2500	Affinity Bioreagents, Golden, CO
αA crystallin	P	1:1000	StressGen, Victoria, BC, Canada
αB crystallin	P	1:2000	Calbiochem, San Diego, CA
FABP-5	P	1:3000	A gift from Dave Bernlohr, Minneapolis, MN
Cofactor A/p14	P	1:4000	A gift from Juan Carlos Zabala, Santander, Spain

* M, monoclonal; P, polyclonal.

2-D Gel Electrophoresis

Conditions for 2-D gel electrophoresis were as described elsewhere.[24] 2-D gels were loaded with 150 μg of retinal protein. The first dimension used a pH 5 to 8 linear gradient (Bio-Rad), and the second dimension was 12% SDS-PAGE. Gels were silver-stained with a MS-compatible kit (BioRad). These conditions were previously determined to be optimal for linearity of most protein spots.

Western Immunoblot of 1-D and 2-D Gels

After 12% SDS-PAGE for either 1-D or 2-D gels, retinal proteins were transferred to polyvinylidene difluoride (PVDF) membranes as previously described.[24,25] For 1-D resolution of protein, the loads used (8–30 μg) were within the linear range of response for each antibody. PVDF membranes were probed with one or more of the primary monoclonal or polyclonal antibodies in Table 1. Goat anti-rabbit, goat anti-mouse, and donkey anti-chicken alkaline phosphatase-conjugated secondary antibodies were used in conjunction with BCIP-NBT (-bromo-4-chloro-3-indoyl phosphate–nitroblue tetrazolium) to visualize immunoreaction. Membranes were imaged (Fluor-S Multi-Imager; Bio-Rad) followed by quantification (Sigma Scan; SPSS, Chicago, IL). All 1-D densities were normalized to a standard used on all blots for comparison, as previously described.[23]

Mass Spectrometry Protein Identification

Preparation and analysis of protein spots for mass spectrometry were as described.[24] Matrix-assisted laser desorption ionization time-of-flight (MALDI-TOF) was performed to obtain peptide mass fingerprints (QSTAR XL quadrupole-TOF mass spectrometer; Applied Biosystems

Downloaded from iovs.arvojournals.org on 08/15/2022

TABLE 2. Donor Demographic

MGS Grade	Donor Distribution			Region Sample Size*		Age (y)		TAD† (h ± SD)	Enu‡ (h ± SD)	Cause of Death§
	Male	Female	Total	M	P	Mean ± SD	Range			
1	9	2	11	8	8	58 ± 12	37–72	17 ± 3	4.7 ± 1.3	Stroke (1), cancer (3), respiratory failure (2), pneumonia (1), hemorrhage (1), head trauma (1), heart failure (2)
2	6	6	12	9	8	70 ± 7	60–83	15 ± 4	4.2 ± 1.6	Cancer (6), respiratory failure (3), pneumonia (1), necrotic bowel (1), stroke (1)
3	7	4	11	9	8	72 ± 8	58–86	18 ± 3	4.9 ± 1.7	Cancer (5), renal failure (1), age (1) heart failure (2), respiratory failure (1), sepsis (1)
4	8	2	10	7	7	82 ± 8	71–94	18 ± 6	4.3 ± 2.3	Heart failure (4), stroke (3), respiratory failure (1), age (1), other (1)

* Donor regions analyzed included the macula (M) and periphery (P).
† Time after death (TAD) until freezing of eye is indicated.
‡ Time after death until enucleation occurred.
§ The number of donors in each cause of death category is shown in parentheses.

Inc. (ABI), Foster City, CA).[24] Peptide peaks were submitted to Mascot (www.matrixscience.com) to obtain initial protein identification. Positive identification was based on a significant Molecular Weight Search (MOWSE) score and mass tolerance less than 50 parts per million.

Confirmation of initial identities was obtained by peptide mass sequencing using either MALDI or electrospray ionization (ESI) MS. Peptides analyzed by ESI were separated by liquid chromatography online (QSTAR Pulsar quadrupole TOF; ABI) and ionized as described.[24]

2-D Gel Analysis

Gel alignment and protein spot densities (spot volume) were quantified (PDQuest software 7.1.1; Bio-Rad) after normalization to total protein load. Automatic spot detection was followed by manual inspection and editing. Log_2-transformed density values were used for statistical analysis.

Statistical Analysis and Selection of Protein Spots for Mass Spectrometry

To determine the number of samples necessary to detect statistically significant changes between groups, a power analysis was performed.[26] The analysis was based on within-group variation in the intensity of individual spots from 2-D gels.

Three models for changes in protein content were tested. In cases in which 2-D gels showed poor spot matching or spots were absent, these data were excluded. Protein levels were screened for patterns that exhibited changes with onset of the disease (change between MGS1 and all other MGS levels), changes that may occur secondarily (changes that occur at MGS4 vs. other levels), and changes that proceed linearly throughout advancing stages of the disease. Because three patterns were tested, a Bonferroni correction was used. Thus, for each test a critical value of 0.017. For both change at onset and end stage, Student's *t*-test was used. Parametric tests for equal variance were used unless there was unequal variance, in which case the parametric Aspin-Welch test was used. In the case of a non-normal distribution, the Whitney-Wilcoxon test was used. To test for linear changes in protein levels, linear regression analysis was performed comparing the stage of MGS. Multiple regression was performed to test for an interaction between age and stage. Our results showed no significant age and stage interaction except for those noted on Table 3.

The same models were tested with the 1-D immunoblot data. However, for two cases (HOP and VDAC in the macula), outliers were removed. One-way ANOVA was performed on times from death until freezing between groups. Linear regression analysis was performed to compare spot density with time from death to freezing. All statistical tests were two sided with $\alpha = 0.05$, unless noted.

RESULTS

Experimental Design

In this study, the macula and periphery of the neurosensory retina were analyzed separately to identify region-specific differences in protein content. Our rationale for this design was based on the preferential deterioration of the macular region in AMD.

The MGS[20] was used to classify donor eyes into four progressive stages (MGS1 to -4). MGS stages are defined by the number and size of yellow deposits (drusen), RPE pigmentary changes, RPE atrophy, and the presence of neovascularization. MGS1 serves as the control group. MGS2 represents early stage AMD, MGS3 is an intermediate stage, and MGS4 is considered end stage (late) AMD. MGS4 is further subdivided into individuals with (exudative AMD) or without (atrophic AMD) neovascularization. In the present study, all MGS4 donors had exudative AMD.

Demographic and clinical information for donor eyes obtained from the Minnesota Lions Eye Bank is summarized in Table 1. The average time to enucleation was 4.5 ± 1.7 hours (mean ± SD, $n = 44$), which is similar to times published in a previous proteome analysis of drusen.[27] After enucleation, eyes were refrigerated until photographing, grading, dissection, and tissue freezing were accomplished. The average time from death to tissue freezing was 16.7 ± 4.4 hours (mean ± SD, $n = 44$). There were no significant differences in time between the four MGS groups. Donors with a known history of diabetes or eye disease other than AMD were excluded from this study. Only eyes from white donors were used in the study.

A minimum of seven samples per region from each MGS category was used. A power analysis based on the variation in intensity of individual spot intensities from 2-D gels indicated that this number was sufficient to detect at least a two-fold change in intensity with 80% power and $\alpha = 0.05$. A total of 584 spots in the macula and 524 spots in the periphery were clearly resolved and analyzed. Linear regression was performed (spot density versus time from death to freezing) to evaluate

Downloaded from iovs.arvojournals.org on 08/15/2022

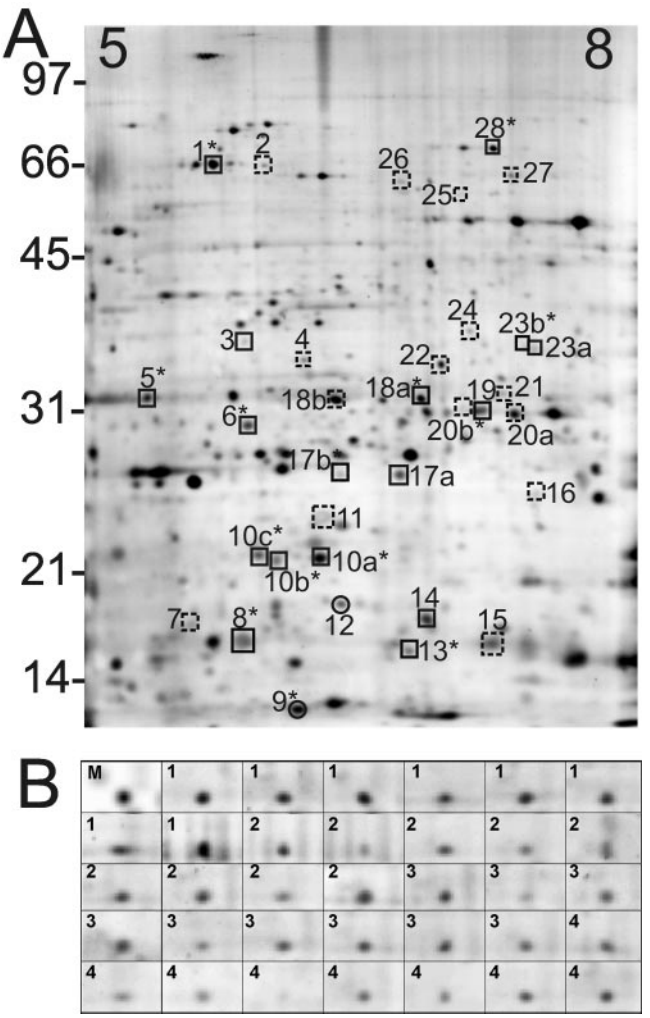

FIGURE 1. Retinal protein resolved by 2-D gel electrophoresis. (**A**) Representative silver-stained gel (150 μg) from the macular region indicates proteins demonstrating altered content with AMD. *Boxed spots* represent identified proteins with altered content in the macula (*solid*) or periphery (*dashed*), or both (*solid with **). *Circles*: unidentified proteins. A linear range of pI 5 to 8 is indicated at the *top*. Molecular weight markers are shown on the *left*. Numbers correspond with proteins in Table 3. (**B**) Spot #18a from the macula of each donor (MGS1 to -4) included in the analysis is shown from the 2-D comparison program. This spot corresponds to a decrease in content with onset (Fig. 1A, Fig. 2C, Table 3). M, the computer-generated master gel used for spot matching.

the postmortem stability of retinal proteins. We found no significant time-dependent change in intensity for >95% of retinal proteins examined, and no change for those spots highlighted in our results. These results indicated no significant degradation occurs within the time scale of our analysis. In addition, replication of eye bank conditions and tissue freezing of rat retinas at time points between 0 and 12 hours resulted in no apparent change in retinal protein content (data not shown). These results indicated proteins from the neurosensory retina are resistant to postmortem changes.

Expression Analysis and Protein Identification

Statistical analyses of spot densities were performed to test three models that describe changes in content at disease onset (early stage, MGS2), linear changes with disease progression, and changes in the late (MGS4) or end stage of the disease (Table 2). Spots changing early or with progression of the disease may reflect potential causal mechanisms. End-stage changes are likely to reflect secondary consequences of the disease. Protein spots with altered levels in either the macula or periphery are indicated in a representative silver-stained gel (Fig. 1A). A representative spot (#18a) demonstrating decreased content at disease onset appeared on all gels included in the macular analysis (Fig. 1B).

Due to the differences in mean ages between MGS stages (Table 2), multiple regression analysis was performed to determine whether age significantly influences the results. With the exception of the proteins noted in Table 3, there was no significant interaction between age and stage. This allows us to conclude that proteins identified in this study are altered specifically due to the stage of disease.

A total of 34 spots changed with MGS category (Figs. 1A, 2, Table 4). Five unique spots in the macula and 15 unique spots in the periphery exhibited region-specific changes in content. Fourteen additional spots either changed significantly in both regions or were significantly altered in one region with a similar trend ($P \leq 0.1$) in the alternate region. One spot (#9) exhibited opposite changes between regions. Thus, while a subset of spots demonstrated region-specific differences, there was significant overlap between the macula and periphery.

Initial protein identities were obtained using MS and confirmed by either tandem MS sequencing of peptides or by a positive immune reaction on 2-D WB (Table 4, Fig. 3). Immune reactions on 2-D WB provided additional information regarding the distribution of spots for each protein and the relative contribution of each isoelectric variant in the population (Fig. 3, Table 5). In most cases, a single protein resolved into multiple protein spots (isoelectric variants). Differences in migration are probably due to posttranslational modification or proteolytic processing that alter the protein's intrinsic charge or size, respectively. When possible, 1-D WB was subsequently performed to provide a semiquantitative measure of protein content for the entire population of isoelectric variants (Fig. 4).

Data regarding protein population distribution and levels are summarized in Table 5. There was good agreement in the direction of change between density on silver stained gels and immune reaction on WB when the spot accounted for most of the proteins. For example, the two protein spots (#17a, #17b), identified as GUK, and accounting for 100% of the population all exhibited decreased density on 2-D gels. This downregulation in macular content was confirmed by WB analysis. In contrast, only one spot (#8), which accounted for ~60% of the multiple isoelectric variants associated with cellular retinoic acid binding protein (CRABP), exhibited decreased macular expression (Fig. 3D). One-dimensional WB showed no significant change in expression suggesting only a subpopulation of CRABP is changing with the disease. These examples highlight the value of using multiple techniques to provide a more comprehensive analysis of protein content.

Region-Specific Expression Changes

Only three proteins with altered content exclusive to the macular region were identified (Fig. 2A, Table 4). Two proteins were altered at onset or with disease progression and one protein exhibited end-stage changes. Ten proteins changed exclusively in the peripheral region (Fig. 2B; Table 4). Seven proteins were altered at onset or with disease progression and three proteins exhibited changes at end stage.

Binding protein (BiP) was identified in a spot (#22) that exhibited decreased content with disease onset. Migration of this spot was at a mass lower than expected for BiP, suggesting proteolysis had occurred. Because only N-terminal peptides were detected in the MS full scan and the spot reacted using an

Downloaded from iovs.arvojournals.org on 08/15/2022

TABLE 3. Statistical Probabilities*

Spot No.	Macular Analysis: Onset: *T*-test 1v234	Macular Analysis: End Stage: *T*-test 123v4	Macular Analysis: Linear: Linear Regression	Peripheral Analysis: Onset: *T*-test 1v234	Peripheral Analysis: End Stage: *T*-test 123v4	Peripheral Analysis: Linear: Linear Regression
1	***0.0023***	**0.0407**	***0.0066***	***0.0063***	—	—
2	—	—	—	—	—	*0.0553*
3	***0.0060***	—	***0.0105***	—	—	—
4	—	—	—	**0.0272**	**0.0308**	***0.0123***
5	***0.0111***	**0.0218**	***0.0020***	*0.0638*	—	—
6	—	**0.0279**	*0.0571*	*0.0872*†	—	—
7	—	—	—	—	***0.0051***	*0.0918*‡
8	—	**0.0438**	**0.0275**	*0.0761*	—	—
9	**0.0260**	—	*0.0865*	*0.0500*	—	—
10a	*0.0917*	*0.0832*	***0.0055***	**0.0400**	—	—
10b	**0.0188**	*0.0923*	**0.0260**	—	**0.0403**	—
10c	*0.0616*	*0.0745*	***0.0084***	*0.0657*	—	—
11	—	—	—	***0.0151***	—	***0.0093***
12	*0.0889*	*0.0541*	***0.0024***	—	—	—
13	*0.0889*	**0.0491**	***0.0096***	**0.0303**	—	—
14	—	***0.0118***	—	—	—	—
15	—	—	—	—	**0.0358**	*0.0652*
16	—	—	—	***0.0094***‡	—	***0.0023***
17a	*0.0813*	*0.0601*	***0.0034***	—	—	—
17b	—	*0.0837*	**0.0183**	—	**0.0050**	*0.0816*
18a	***0.0087***	—	**0.0286**	***0.0039***	—	***0.0124***
18b	—	—	—	***0.0160***	—	—
19	—	—	—	***0.0044***	**0.0447**†	***0.0097***†
20a	—	—	—	*0.0543*	*0.0936*	—
20b	**0.0477**	*0.0562*	**0.0188**	—	**0.0499**	*0.0763*
21	—	—	—	—	**0.0278**	**0.0318**
22	—	—	—	***0.0028***	—	—
23a	—	***0.0077***	*0.0548*	—	—	—
23b	—	**0.0395**	***0.0142***	***0.0063***	—	**0.0254**
24	—	—	—	**0.0293**	—	**0.0438**
25	—	—	—	—	***0.0026***	**0.0435**
26	—	—	—	**0.0325**	—	**0.0212**
27	—	—	—	***0.0140***	—	—
28	***0.0001***	**0.0322**	***0.0048***	*0.0901*	—	—

* $P \leq 0.1$ (italics) indicate a significant trend; $P \leq 0.05$ (bold) indicate significance, $P \leq 0.017$ (bold italics) indicate significance when adjusted for testing multiple models.

† Only a significant age-dependent change using multiple regression.

‡ Both age and stage are significant factors, as tested by multiple regression.

N-terminal antibody, BiP truncation probably occurred at the C terminus. The consistent presence of truncated BiP in the neurosensory retina may have currently unknown but biologically relevant consequence.

Expression Changes Common to both Macula and Periphery

Twelve proteins exhibited either significant changes in content for both regions or were significantly altered in one region with a trend ($P \leq 0.1$) in the alternate region (Table 4). We report trends because they may provide biologically meaningful information about the sequence of region-specific changes during disease progression. Ten proteins were altered at onset or with disease progression, and two proteins were altered at end stage.

Content of endoplasmic reticulum protein 29 (ERp29) was altered at disease onset according to the 2-D gel analysis (Fig. 2C). Semiquantitative 1-D WB revealed no significant differences in immune reaction between MGS stages (Fig. 4, Table 5). A nonsignificant change in total density of this protein was not surprising, given that only one spot (#18a), accounting for 33% of the total ERp29, exhibited altered content. However, in the periphery, both isoelectric variants (#18a, #18b), accounting for 100% of the population, showed decreased levels. A possible explanation for the observed anomaly is that ERp29 is a soluble protein that is located in the endoplasmic reticulum. The difference in results from 2-D and 1-D gels may reflect the reduced solubility of a protein localized inside an organelle that would limit its ability to resolve in the first dimension during 2-D gel electrophoresis.

Another conflict between 2-D and 1-D analyses was observed for αA crystallin. The majority (~98%) of αA crystallin migrated as a single spot (#11) (Fig. 3C; Table 5). The immune reaction on 1-D WB exhibited increased levels in the macula ($P = 0.004$; Figs. 4A, 4B). However, 2-D gel analysis showed decreased density of the major αA crystallin spot in the periphery. The apparent decrease in density on 2-D gels could be due to irregular staining of this protein, a property unique to silver staining of glycosylated proteins.[28] Therefore, the immune reaction on 1-D WB is likely to provide a more valid measure of the total content of this protein.

DISCUSSION

In the present study, we performed a global protein analysis on the macula and periphery of the neurosensory retina from

Downloaded from iovs.arvojournals.org on 08/15/2022

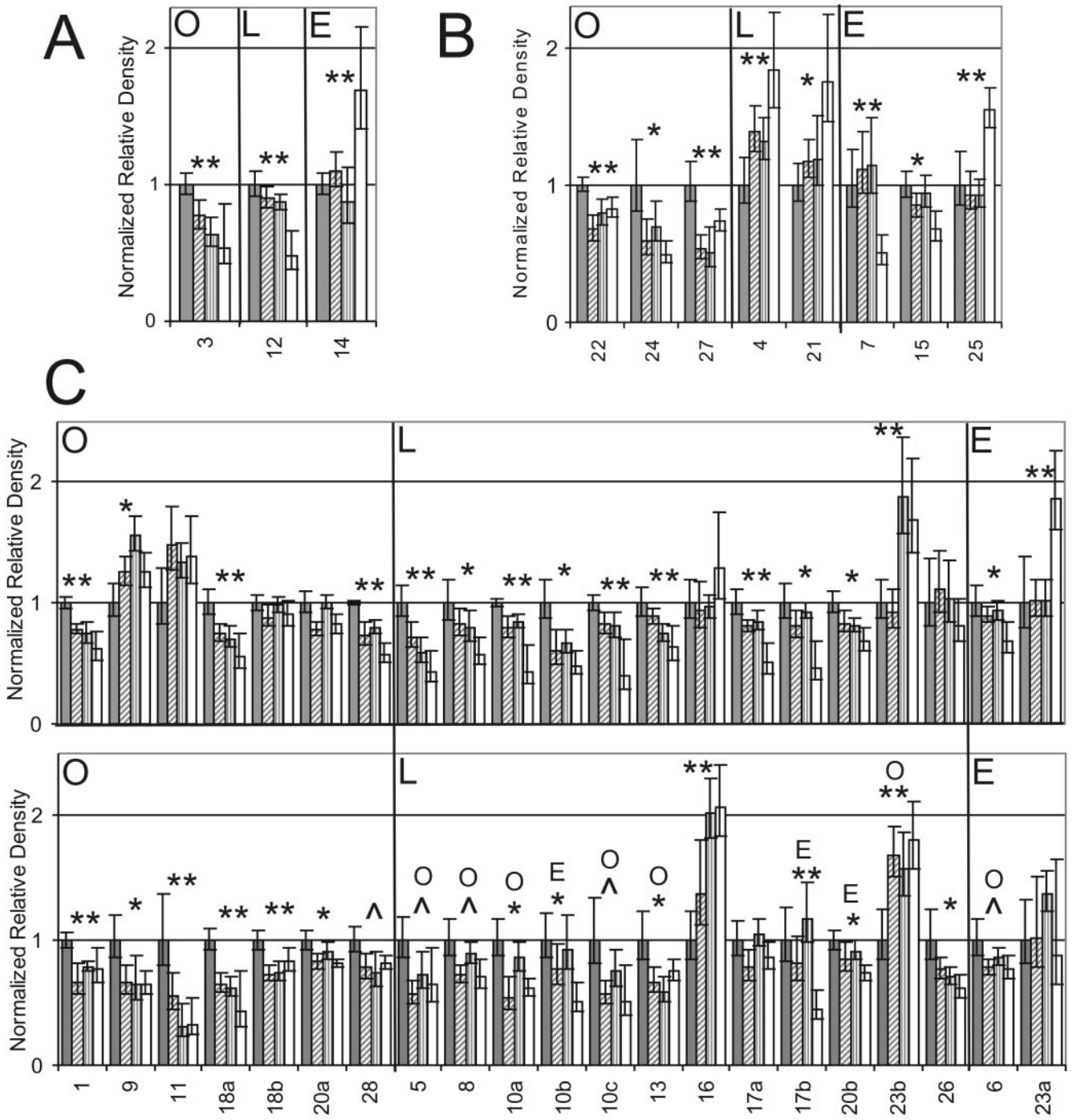

FIGURE 2. Summary of protein spots with altered protein levels. Results of densitometry for protein spots on 2-D gels demonstrating changes at onset (O), linearly (L), or at end stage (E) of AMD in the macula (**A**), periphery (**B**), or both (**C**) regions of the retina. (**C**) *Top* and *bottom*: data from the macula and periphery, respectively, for the corresponding protein spots between each region. O, L, E above the bars: spot density fits a model of change differing from that in the alternate region. Data are the mean (± SEM) spot densities for MGS1 (*gray*), MGS2 (*hatched*), MGS3 (*vertical*), MGS4 (*white*) that were normalized to MGS1. Asymmetric error bars: back-transformed density values from $\log_2$. Spots #2 and #19 are not represented. $^{**}P \leq 0.017$ (significance adjusted for testing 3 models), $^{*}P \leq 0.05$, $^{\wedge}P \leq 0.1$. All probabilities (including #2 and #19) are listed in Table 3. $n = 4$ to 9 observations/level.

donor eyes categorized for AMD using the MGS for postmortem eye bank tissue.[20] By using the MGS in conjunction with proteomics, we identified significant region-specific changes in protein content at distinct stages of AMD. Furthermore, examination of postmortem donor eyes allowed us to study the human disease process directly.

In a parallel study performed in our laboratory, we analyzed the proteome of RPE from donor eyes categorized using the MGS.[29] Comparison of the major results from the RPE and neurosensory retina shows a significant decline in chaperones and stress-related proteins early in the disease. In contrast, there were several changes unique to each tissue. For example,

Downloaded from iovs.arvojournals.org on 08/15/2022

TABLE 4. Protein Identification

Spot No.	Region*†	Model‡	Direction§	Protein‖	Accession No. (gi)	Theoretical MW(kDa)/ pI	MALDI-TOF MS		MSMS No. Peptides	Immune Reaction
							No. Peptides	% Coverage		
1	M/P	O/O	D/D	HSP (heat shock protein) 60	306809	61.2/5.7	13	28	2	X
2	tP	L	I	TCP-1ε	23273788	60.1/5.5	15	42		
3	M	O	D	Glyoxalase	16198390	33.5/5.4	7	23	2	
4	P	L	I	α-Enolase	2979261	47.5/7.0	10	36	2	X¶
5	M(tP)	L/O	D/D	Calretinin	4502543	31.6/5.1	17	62	1	X¶
6	M(tP)	E/O	D/D	UCH-L1	21361091	25.2/5.3	10	54	2	X¶
7	P	E	D	Cofactor a	30583547	12.9/5.3	6	40	3	X
8	M(tP)	L/O	D/D	CRABP	4758052	15.7/5.3	10	69	2	X
9	M/P	O/O	I/D	ND						
10a	M/P	L/O	D/D	Stathmin	15680064	17.3/5.8	5	42	3	X
10b	M/P	O/E	D/D	Stathmin	15680064	17.3/5.8	3	32	1	X
10c	M(tP)	L/O	D/D	Stathmin	15680064	17.3/5.8	2	18	1	X
11	P	L	D	αA crystallin	46854599	20.0/5.8	12	61	2	X
12	M	L	D	ND						
13	M/P	L/O	D/D	Prefoldin	3212110	14.2/6.3	2	19	2	X
14	M	E	I	FABP-5	30583737	15.5/6.6	9	65	2	X
15	P	E	D	HIT protein 1	3114502	13.9/6.2	5	57	1	
16	P	L	I	αB crystallin	30582379	20.1/6.8	8	38	2	X
17a	M	L	D	GUK	55959192	23.7/6.9	5	25	2	X
17b	M/P	L/E	D/D	GUK	55959192	23.7/6.9	7	46	1	X
18a	M/P	O/O	D/D	ERp29	5803013	29.0/6.8	13	59	3	X
18b	P	O	D	ERp29	5803013	29.0/6.8	10	42	2	X
19	P	O	I	α1 proteasome	55640605	27.8/6.3	11	44	4	
20a	tP	O	D	TPI	136066	26.9/6.5	9	47	2	
20b	M/P	L/E	D/D	TPI	136066	26.9/6.5	15	73	7	
21	P	L	I	HSP70i2 variant	62896815	53.6/5.6	6	18	1	
22	P	O	D	BiP	6470150	71.0/5.2	13	23	1	X¶
23a	M	E	I	VDAC1	238427	30.9/8.6	10	55	1	X
23b	M/P	L/O	I/I	VDAC1	238427	30.9/8.6	10	55	3	X
24	P	O	D	α-Enolase	2979261	47.5/7.0	16	40	1	X
24	P	O	D	Aldolase C	30582851	39.8/6.4	13	51	1	
25	P	E	I	Leucine aminopeptidase	12643394	53.1/6.3	14	38	1	
26	P	L	D	OXCT	10280560	56.6/7.1	7	24	1	
26	P	L	D	α-Tubulin	37492	50.8/5.0	8	28	1	
27	P	O	D	Dihydrolipoamide dehydrogenase	181575	54.7/8.0	10	34	2	
28	M(tP)	O/O	D/D	HOP	12804257	63.2/6.4	25	46	4	X

* Region includes the macula (M) and periphery (P).
† All regions listed have $P \leq 0.05$ except for those indicated that show a significant trend (tP or tM) in a given region $P \leq 0.1$.
‡ Models include onset (O), linear (L) and end stage (E).
§ Direction includes increased (I) or decreased (D) expression in the regions indicated.
‖ ND refers to proteins not determined with MS.
¶ Immune reactions on 2D WB not shown in Figure 3.

the RPE exhibited altered content of several proteins involved in mitochondrial protein trafficking and refolding, whereas results from the neurosensory retina strongly indicated the microtubule pathway was affected. Thus, results from our coordinated proteome analysis of both the neurosensory retina and RPE highlights the importance of studying both tissues of the retina to provide a more comprehensive understanding of the disease process.

There are several important outcomes of this study. First, this global investigation of protein changes narrows the focus to specific proteins and pathways that may play a key role in the disease process. This information provides a rational basis for in-depth studies to investigate the consequences of altering the content of specific retinal proteins and pathways. Second, because the four MGS stages correspond with the classification of AMD described in the AREDS report,[21] our results are applicable to large clinical trials and epidemiologic studies that use the AREDS definitions. This should facilitate translation of our findings at the molecular level to the clinical disease. Finally, the pattern of protein change may help distinguish between potential causal mechanisms (changes occurring linearly or at disease onset) from secondary effects of the disease (changes occurring at end stage). This information could eventually be used to develop pharmacotherapies targeted at the fundamental biochemical defects and attenuate disease progression before vision loss.

Our experimental approach used high-resolution 2-D gel protein analysis, MS, 1-D and 2-D WB to provide a more comprehensive analysis of protein-specific changes that occur with AMD. The use of 2-D WB helped identify the distribution of spots associated with specific proteins that may reflect functionally distinct subpopulations. Isoelectric variants can reflect either proteolytic processing or changes in intrinsic charge due to posttranslational modifications. For some proteins, isoelectric variants have been shown to alter protein function or subcellular localization.[30] Conversely, changes in a subpopula-

Downloaded from iovs.arvojournals.org on 08/15/2022

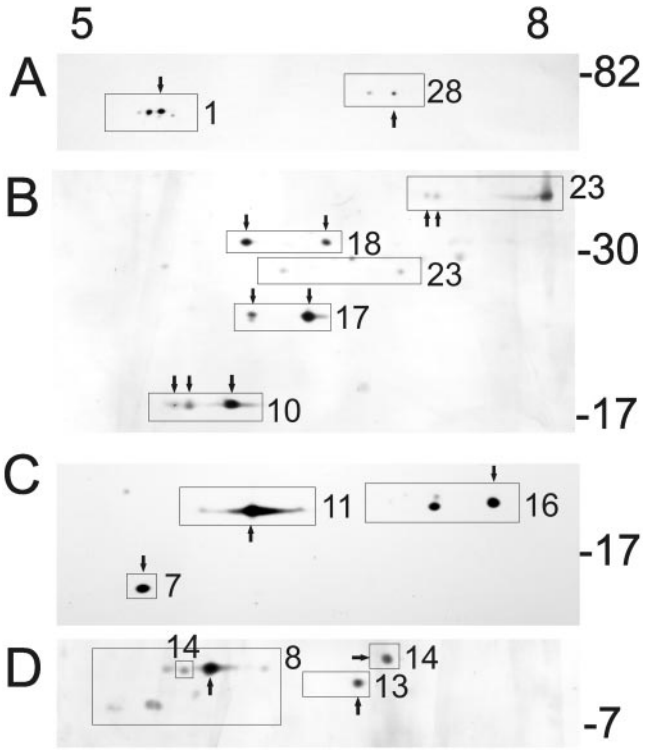

FIGURE 3. Immune reactive spots on 2-D WB identified protein-specific distributions. Protein (150 μg) resolved by 2-D electrophoresis was transferred and probed with antibodies to specific proteins including HSP60 (#1) and HOP (#28) (**A**), VDAC1 (#23), GUK (#17), ERp29 (#18), and Stathmin (#10) (**B**), aA crystallin (#11), aB crystallin (#16), cofactor a (#7) (**C**), CRABP (#8), prefoldin (#13), and FABP5 (#14) (**D**). Blots were stripped between antibodies and reprobed. Numbers correspond with proteins listed in Table 4. *Arrows*: spots with altered content determined on 2-D gels. A linear range of pI 5 to 8 is indicated at the *top*. Migration of molecular weight markers are shown on the *right*.

tion of spots that constitute only a minor portion of the total population may have little impact. Thus, the functional significance of protein changes limited to a subpopulation will require further study. 1-D WB provided an estimate of the total content of specific proteins and helped distinguish protein-specific changes in content. In addition, 1-D WB provided a valid alternative method for the use of density on silver-stained gels to estimate the content of proteins that stain irregularly, such as seen with αA crystallin.

Several limitations inherent to 2-D gel resolution have influenced our results. Although this technique provides superior resolution of soluble proteins, most membrane proteins are not resolved in the first dimension and consequently are not present on 2-D gels. Proteins in low abundance are often below the detection limit and would be poorly represented in this analysis. Resolution in the first dimension is limited by the selection of the pH range. In the present study, we used a pH range of 5 to 8 because it provided optimal resolution of the greatest number of proteins. The low number of samples included in each group would also limit our ability to find statistically significant differences in content. Considering these caveats, the number of proteins identified in the present study is a conservative estimate of the actual number changing with AMD.

Approximately 60% of the proteins identified as having altered content in this study exhibited region-specific changes in protein levels. The remaining 40%, including proteins demonstrating trends in alternate regions, exhibited changes common to both regions. The clinical observation of accelerated degeneration of the macula with AMD suggests that molecular changes occur predominantly in the macula. Our data do not support this idea, since only ~10% of the total protein changes identified were exclusive to the macula. It appears that the disease also impacts the peripheral retina. Clinical data that support results from the current proteomic analysis have shown degeneration of the peripheral retina concomitant with macular degeneration.[31] Another study reported ~20% of patients with AMD present features, such as drusen and geographic atrophy, in both the macula and periphery.[32] A more recent study suggested that this global manifestation of the disease may reflect a genetic component behind retinal cell dysfunction since peripheral features, such as drusen, exhibited a familial linkage.[32,33] Therefore, the accelerated degeneration of the macula is probably due to a combination of genetics, and the unique features (concentrated light energy and highly oxygenated tissues) that make this region more susceptible to environmental insults.

Our analysis of protein content revealed 26 proteins changing during the progression of AMD. Two groups of functionally linked proteins are particularly interesting. One group (tubulin, prefoldin-1, TCP-1, cofactor a, stathmin) is involved in microtubule formation and regulation. These proteins exhibit a pattern of decreased protein levels (at onset or linearly) suggesting their involvement in the early pathogenesis of AMD. Formation of microtubules requires tubulin, the main component of microtubules, to interact with several cofactors, including cofactor a.[34] Interaction of tubulin with chaperone complexes that include prefoldin-1 and TCP-1, involved in tubulin transport and folding, is also necessary for microtubule assembly.[35,36] Stathmin regulates the process of microtubule remodeling that is involved in maintaining retinal plasticity and during retinal regeneration.[37,38] Decreased expression of stathmin has also been reported with neurodegenerative diseases such as Alzheimer's.[37] The diminished levels of proteins involved in microtubule formation could result in a loss of retinal plasticity and regenerative capacity.

Although microtubule proteins are globally expressed in all cells of the neurosensory retina, a large concentration of microtubules is present in the photoreceptors where they facilitate protein transport between the inner and outer segments. A disturbance in the microtubule-based cytoskeleton within photoreceptor outer segments may contribute to a loss of photoreceptors.[9] Because the greatest photoreceptor loss occurs in the macula,[14,23] it is reasonable to postulate that the decreased levels of microtubule proteins corresponds directly to the disease-induced loss in photoreceptors. However, our data showed a significant decrease in content of microtubule proteins in both regions suggesting that changes are not exclusive to photoreceptors. However, because our neurosensory retina preparation contains photoreceptors in addition to six other retinal cell types, we cannot discriminate the exact cellular site of altered protein levels.

A second group of functionally linked proteins demonstrating altered protein levels with progressive AMD are the chaperones HOP, HSP60, αA crystallin, and αB crystallin. HOP and mitochondrial HSP60 content was downregulated, whereas Western blot analysis showed that protein levels of αA crystallin and αB crystallin were upregulated. HOP is a promiscuous cochaperone that modulates the activity of HSP70 and HSP90 in protein folding.[39] HSP60 is localized to the mitochondria, where it participates in the trafficking and folding of mitochondrial matrix proteins.[40] αA- and αB-crystallin are small heat shock proteins that protect against aggregation of partially unfolded proteins. Upregulation may reflect a cellular response to oxidative stress.[41,42] The chaperones identified in this study

Downloaded from iovs.arvojournals.org on 08/15/2022

Downloaded from iovs.arvojournals.org on 08/15/2022

TABLE 5. Protein Distribution and Expression

		Macula							Periphery						
Spot No.	Protein	2D WB (%)	No. Spots	2D Gel Pattern†‡	2D Gel Direction§	1D WB Pattern	1D WB Direction	1D *P* Value	2D WB (%)	No. Spots	2D Gel Pattern†‡	2D Gel Direction§	1D WB Pattern	1D WB Direction	1D *P* Value
Macula															
14	FABP	−65	2	E	I	—									
Periphery															
4	α-enolase								<5¶	many¶	O	I	—		
7	cofactor a								100	1	E	D	—		
22	BiP								<30¶	many¶	O	D	—		
24	α-enolase								<5¶	many¶	O	D	—		
24	aldolase C								<5‖	many‖	O	D	—		
Common to both															
1	HSP60	−50	5	O	D	—			−50	5	O	D	—		
5	calretinin	>90	2¶	L	D	—			>90	2¶	O(t)	D	—		
8	CRABP	60	many	L	D	NC		0.713	60	many	O(t)	D	—		
10a,b,c	stathmin	100	3	L&O	D	O(t)	D	0.063	100	3	O&E	D	—		
11	αA	>98	3	NC		L	I	0.004	>98	3	L	D	NC		0.360
13	prefoldin	>98	2	L	D	NC		0.264	>98	2	O	D	NC		0.252
16	αB	−50	5	NC		L	I	0.047	50	5	L	I	L	I	0.003
17a,b	GUK	100	2	L	D	L	D	0.002	22	2	E	D	NC		0.194
18a,b	ERp29	−33	2	O	D	NC		0.629	100	2	O	D	NC		0.506
20a,b	TPI	−20‖	many‖	L	D	—			−30‖	many‖	O&E	D	—		
23a,b	VDAC	−10	5	E&L	I	L	D	0.026	<10	5	O	I	NC		0.381
26	α-tubulin	—	many¶	NC		L	D	0.056	—	many¶	L	D	L	D	0.006
28	HOP	−65	2	O	D	L	D	0.015	−65	2	O(t)	D	—		

* Protein abbreviations: CRABP (cellular retinoic acid-binding protein), FABP (fatty acid binding protein), HOP (heat shock protein 70/90 organizing protein), BiP (binding protein), αA (αA crystallin), αB (αB crystallin), GUK (guanylate kinase), ERp29 (endoplasmic reticulum protein 29), TPI (triose phosphate isomerase), VDAC (voltage-dependent anion channel 1).

† Expression pattern includes onset (O), linear (L) and end stage (E).

‡ (t) indicates a trend ($P \leq 0.1$).

§ Direction includes increased (I) or decreased (D) expression.

‖ Determined by MS.

¶ data for 2D WB not shown in Figure 3. NC, no change.

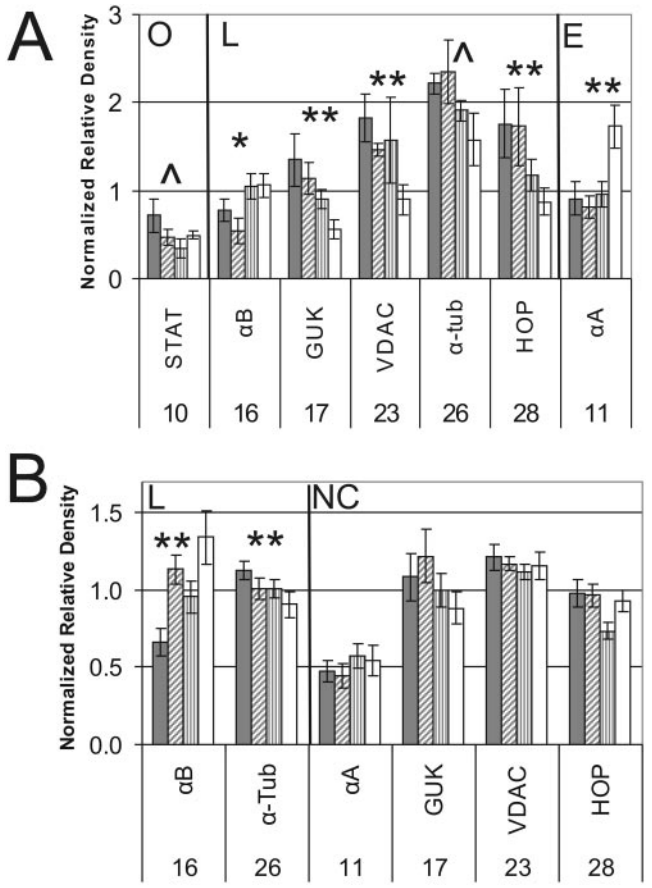

FIGURE 4. Semiquantitative analysis of protein levels by 1-D WB. Densitometric analysis of immune reactions for proteins resolved on 1-D WB demonstrating no change (NC) or changes at onset (O), linearly (L), or at end stage (E) of AMD in the macula (**A**) and periphery (**B**) of the retina. Data are the mean (± SEM) densities of immune reactions for MGS1 (*gray*), MGS2 (*hatched*), MGS3 (*vertical*), MGS4 (*white*) bars. $^{**}P \leq 0.017$ (significance adjusted for testing three models), $^{*}P \leq 0.05$, $^{\wedge}P \leq 0.1$. Abbreviations for antibodies: STAT (stathmin), αA (αA crystallin), αB (αB crystallin), GUK (guanylate kinase), VDAC (voltage-dependent anion channel 1), α-tub (α-tubulin), HOP (heat shock protein70/90 organizing protein). $n = 3$ to 14 and $n = 2$ to 12 donors per level within the periphery and macula, respectively.

may be mechanistically involved in AMD pathogenesis through their role in regulating apoptotic cell death.[43]

Because AMD is a multifaceted disease that probably reflects complex relationships between several pathophysiological pathways, diverse experimental approaches are necessary for thoroughly examining the underlying cellular processes. For example, the identification of complement factor H polymorphisms associated with AMD built on several lines of evidence obtained from distinct approaches including immunohistochemistry,[44] human genetics,[45–48] and proteomic analysis of drusen.[27] In a parallel example from our own study, we found downregulation of GUK, a protein that is involved in the cGMP cycle required for phototransduction. Genetic analysis also implicated GUK as a candidate gene linked to AMD and other retinal degenerations.[49]

In summary, the biochemical changes identified in the present study represent novel contributions toward understanding AMD pathophysiology. Our proteomic analysis identified regional changes at all stages of the disease, including those that precede vision loss. These results further elucidate the molecular basis of AMD, a requisite step in designing therapeutic approaches that attenuate disease progression.

Acknowledgments

The authors thank the Minnesota Lions Eye Bank for their assistance in procuring eyes for this study; Juan Carlos Zabala and Dave Bernlohr for kind gifts of antibodies; Curt Nordgaard for assistance in manuscript preparation and revision; and Kathleen Lew, Nabamita Basak, Kristin Pilon, Kristin Berg, and the Mass Spectrometry Consortium for the Life Sciences at the University of Minnesota for technical assistance.

References

1. Klein R, Klein BE, Linton KL. Prevalence of age-related maculopathy. The Beaver Dam Eye Study. *Ophthalmology*. 1992;99:933–943.
2. Leibowitz HM, Krueger DE, Maunder LR, et al. The Framingham Eye Study monograph: an ophthalmological and epidemiological study of cataract, glaucoma, diabetic retinopathy, macular degeneration, and visual acuity in a general population of 2631 adults, 1973–1975. *Surv Ophthalmol*. 1980;24:335–610.
3. Verteporfin in Photodynamic Therapy Study Group. Verteporfin therapy of subfoveal choroidal neovascularization in age-related macular degeneration: two-year results of a randomized clinical trial including lesions with occult with no classic choroidal neovascularization–verteporfin in photodynamic therapy report 2. *Am J Ophthalmol.* 2001;131:541–560.
4. Treatment of Age-related Macular Degeneration with Photodynamic Therapy (TAP) Study Group. Photodynamic therapy of subfoveal choroidal neovascularization in age-related macular degeneration with verteporfin: one-year results of 2 randomized clinical trials–TAP report. *Arch Ophthalmol.* 1999;117:1329–1345.
5. Gragoudas ES, Adamis AP, Cunningham ET Jr, Feinsod M, Guyer DR. Pegaptanib for neovascular age-related macular degeneration. *N Engl J Med*. 2004;351:2805–2816.
6. Spraul CW, Lang GE, Grossniklaus HE, Lang GK. Histologic and morphometric analysis of the choroid, Bruch's membrane, and retinal pigment epithelium in postmortem eyes with age-related macular degeneration and histologic examination of surgically excised choroidal neovascular membranes. *Surv Ophthalmol.* 1999;44(suppl 1):S10–S32.
7. Bhutto IA, McLeod DS, Hasegawa T, et al. Pigment epithelium-derived factor (PEDF) and vascular endothelial growth factor (VEGF) in aged human choroid and eyes with age-related macular degeneration. *Exp Eye Res.* 2006;82:99–110.
8. Martin G, Schlunck G, Hansen LL, Agostini HT. Differential expression of angioregulatory factors in normal and CNV-derived human retinal pigment epithelium. *Graefes Arch Clin Exp Ophthalmol*. 2004;242:321–326.
9. Eckmiller MS. Defective cone photoreceptor cytoskeleton, alignment, feedback, and energetics can lead to energy depletion in macular degeneration. *Prog Retin Eye Res.* 2004;23:495–522.
10. Zarbin MA. Current concepts in the pathogenesis of age-related macular degeneration. *Arch Ophthalmol.* 2004;122:598–614.
11. Owsley C, Jackson GR, Cideciyan AV, et al. Psychophysical evidence for rod vulnerability in age-related macular degeneration. *Invest Ophthalmol Vis Sci*. 2000;41:267–273.
12. Owsley C, Jackson GR, White M, Feist R, Edwards D. Delays in rod-mediated dark adaptation in early age-related maculopathy. *Ophthalmology*. 2001;108:1196–1202.
13. Jackson GR, Owsley C, Curcio CA. Photoreceptor degeneration and dysfunction in aging and age-related maculopathy. *Ageing Res Rev*. 2002;1:381–396.
14. Curcio CA, Millican CL, Allen KA, Kalina RE. Aging of the human photoreceptor mosaic: evidence for selective vulnerability of rods in central retina. *Invest Ophthalmol Vis Sci*. 1993;34:3278–3296.
15. Gorin MB, Jackson KE, Ferrell RE, et al. A peripherin/retinal degeneration slow mutation (Pro-210-Arg) associated with macular and peripheral retinal degeneration. *Ophthalmology*. 1995;102:246–255.
16. Cahill MT, Mruthyunjaya P, Bowes Rickman C, Toth CA. Recurrence of retinal pigment epithelial changes after macular translocation with 360 degrees peripheral retinectomy for geographic atrophy. *Arch Ophthalmol*. 2005;123:935–938.

Downloaded from iovs.arvojournals.org on 08/15/2022

17. Khurana RN, Fujii GY, Walsh AC, Humayun MS, de Juan E Jr, Sadda SR. Rapid recurrence of geographic atrophy after full macular translocation for nonexudative age-related macular degeneration. *Ophthalmology*. 2005;112:1586–1591.
18. Simon P, Glacet-Bernard A, Coscas G, Soubrane G. Progression of choroidal neovascularization after macular translocation in age-related macular degeneration and degenerative myopia [in French]. *J Fr Ophtalmol*. 2002;25:694–700.
19. Ambati J, Ambati BK, Yoo SH, Ianchulev S, Adamis AP. Age-related macular degeneration: etiology, pathogenesis, and therapeutic strategies. *Surv Ophthalmol*. 2003;48:257–293.
20. Olsen TW, Feng X. The Minnesota Grading System of eye bank eyes for age-related macular degeneration. *Invest Ophthalmol Vis Sci*. 2004;45:4484–4490.
21. The Age-Related Eye Disease Study system for classifying age-related macular degeneration from stereoscopic color fundus photographs: the Age-Related Eye Disease Study Report Number 6. *Am J Ophthalmol.* 2001;132:668–681.
22. Klein R, Davis MD, Magli YL, Segal P, Klein BE, Hubbard L. The Wisconsin age-related maculopathy grading system. *Ophthalmology*. 1991;98:1128–1134.
23. Ethen CM, Feng X, Olsen TW, Ferrington DA. Declines in arrestin and rhodopsin in the macula with progression of age-related macular degeneration. *Invest Ophthalmol Vis Sci*. 2005;46:769–775.
24. Kapphahn RJ, Ethen CM, Peters EA, Higgins L, Ferrington DA. Modified alpha A crystallin in the retina: altered expression and truncation with aging. *Biochemistry*. 2003;42:15310–15125.
25. Laemmli UK. Cleavage of structural proteins during the assembly of the head of bacteriophage T4. *Nature.* 1970;227:680–685.
26. Ferrington DA, Krainev AG, Bigelow DJ. Altered turnover of calcium regulatory proteins of the sarcoplasmic reticulum in aged skeletal muscle. *J Biol Chem*. 1998;273:5885–5891.
27. Crabb JW, Miyagi M, Gu X. Drusen proteome analysis: an approach to the etiology of age-related macular degeneration. *Proc Natl Acad Sci USA*. 2002;99:14682–14687.
28. Merril CR, Washart KM. Protein detection methods. In: Hames BD, ed. *Gel Electrophoresis of Proteins.* New York: Oxford University Press, Inc.; 1998:57–61.
29. Nordgaard CL, Berg KM, Kapphahn RJ, et al. Proteomics of the retinal pigment epithelium reveals altered protein expression at progressive stages of age-related macular degeneration. *Invest Ophthalmol Vis Sci.* 2006;47:815–822.
30. Means GE, Feeney RE, Martin BL. Chemical and post-translational modification of proteins. In: Chambers JA, Rickwood D, eds. *Biochemistry*. Oxford, UK: BIOS Scientific Publishers Limited, Oxford, 1993:215–245.
31. Lewis H, Straatsma BR, Foos RY, Lightfoot DO. Reticular degeneration of the pigment epithelium. *Ophthalmology*. 1985;92:1485–1495.
32. Postel EA, Agarwal A, Schmidt S, et al. Comparing age-related macular degeneration phenotype in probands from singleton and multiplex families. *Am J Ophthalmol*. 2005;139:820–825.
33. Traboulsi EI. The challenges and surprises of studying the genetics of age-related macular degeneration. *Am J Ophthalmol.* 2005;139:908–911.
34. Lopez-Fanarraga M, Avila J, Guasch A, Coll M, Zabala JC. Review: postchaperonin tubulin folding cofactors and their role in microtubule dynamics. *J Struct Biol*. 2001;135:219–229.
35. Cowan NJ, Lewis SA. Type II chaperonins, prefoldin, and the tubulin-specific chaperones. *Adv Protein Chem*. 2001;59:73–104.
36. Vainberg IE, Lewis SA, Rommelaere H, et al. Prefoldin, a chaperone that delivers unfolded proteins to cytosolic chaperonin. *Cell*. 1998; 93:863–873.
37. Mori N, Morii H. SCG10-related neuronal growth-associated proteins in neural development, plasticity, degeneration and aging. *J Neurosci Res*. 2002;70:264–273.
38. Nakazawa T, Nakano I, Furuyama T, Morii H, Tamai M, Mori N. The SCG10-related gene family in the developing rat retina: persistent expression of SCLIP and stathmin in mature ganglion cell layer. *Brain Res*. 2000;861:399–407.
39. Odunuga OO, Longshaw VM, Blatch GL. Hop: more than an Hsp70/Hsp90 adaptor protein. *Bioessays*. 2004;26:1058–1068.
40. Voos W, Rottgers K. Molecular chaperones as essential mediators of mitochondrial biogenesis. *Biochim Biophys Acta*. 2002;1592: 51–62.
41. Horwitz J. Alpha-crystallin can function as a molecular chaperone. *Proc Natl Acad Sci USA.* 1992;89:10449–10453.
42. Golenhofen N, Ness W, Wawrousek EF, Drenckhahn D. Expression and induction of the stress protein alpha-B-crystallin in vascular endothelial cells. *Histochem Cell Biol*. 2002;117:203–209.
43. Parcellier A, Gurbuxani S, Schmitt E, Solary E, Garrido C. Heat shock proteins, cellular chaperones that modulate mitochondrial cell death pathways. *Biochem Biophys Res Commun*. 2003;304: 505–512.
44. Hageman GS, Mullins RF. Molecular composition of drusen as related to substructural phenotype. *Mol Vis*. 1999;5:28.
45. Edwards AO, Ritter R 3rd, Abel KJ, Manning A, Panhuysen C, Farrer LA. Complement factor H polymorphism and age-related macular degeneration. *Science*. 2005;308:421–424.
46. Hageman GS, Anderson DH, Johnson LV, et al. A common haplotype in the complement regulatory gene factor H (HF1/CFH) predisposes individuals to age-related macular degeneration. *Proc Natl Acad Sci USA*. 2005;102:7227–7232.
47. Haines JL, Hauser MA, Schmidt S, et al. Complement factor H variant increases the risk of age-related macular degeneration. *Science*. 2005;308:419–421.
48. Klein RJ, Zeiss C, Chew EY, et al. Complement factor H polymorphism in age-related macular degeneration. *Science*. 2005;308: 385–389.
49. Fitzgibbon J, Katsanis N, Wells D, Delhanty J, Vallins W, Hunt DM. Human guanylate kinase (GUK1): cDNA sequence, expression and chromosomal localisation. *FEBS Lett*. 1996;385:185–188.

Downloaded from iovs.arvojournals.org on 08/15/2022